4586 J. Phys. Chem. 1985, 89, 4586-4591

Thermal Unimolecular Decomposition of Nitrous Oxide at Low Pressures

Hélène Loirat, Françoise Caralp,

Laboratoire de chimie physique, Université de Bordeaux I, 33405 Talence Cedex, France

Wendell Forst,* and Christian Schoenenberger

Department of Chemistry and C.R.A.M., Laval University, Quebec, Canada G1K 7P4
(Received: March 13, 1985)

The thermal decomposition of nitrous oxide, pure and in mixtures with N_2 and CO_2, was studied in a quartz vessel in the temperature range from 1080 to 1227 K at concentrations ranging from 10^{-7} to 1.5×10^{-6} mol/cm^3, the lowest of which represents a concentration almost two orders of magnitude lower than in most previous studies. It is found that the activation energy, based on both the raw experimental data and data corrected for heterogeneity, shows continued falloff with pressure with no indication of reaching a limit at the lowest pressure studied. This is in accord with the prediction of the theory of Lorquet, Lorquet, and Forst (LLF), and in considerable disagreement with the recommended values of Baulch et al. The LLF theory reproduces fairly well the experimental concentration dependence of both the rate constant and activation energy, but experiment seems to indicate that activation energy may fall off with pressure somewhat faster than predicted by theory.

1. Introduction

Nitrous oxide is a molecule of considerable interest, both practical and theoretical. On the practical side, nitrous oxide is often used as an oxidant, more specifically as a source of oxygen atoms. From the theoretical point of view, the interest in nitrous oxide is due to the fact that N_2O is the smallest molecule whose decomposition involves two potential energy surfaces of different multiplicities. For all these reasons, the decomposition of N_2O has been the subject of numerous experimental studies over the years,[1-3,5] as well as of a number of theoretical calculations.[4]

In a thermal system, the rate of the elementary decomposition

$$N_2O(^1\Sigma) \rightarrow N_2(^1\Sigma) + O(^3P) \qquad \text{(I)}$$

shows a falloff with pressure typical of a thermal unimolecular reaction. While there appears to be a consensus insofar as the limiting high-pressure rate constant (k_∞) is concerned, there is less agreement regarding the rate, and particularly the activation energy, at low pressures. Figure 1 and Table I summarize existing data. The figure is adapted from one published in 1973 by Baulch et al.,[5] to which were added new results that became available since, including those of the present study.

More recently, one of us[6] has reviewed the then existing low-pressure N_2O rate data in the light of the theory of Lorquet, Lorquet, and Forst (LLF)[4] which predicts[6] that both the (pressure-dependent) rate constant k_{uni}, and especially the associated activation energy E_a, should keep falling off with pressure, essentially "forever". The experimental evidence available at the time in support of this prediction was ambiguous: while no experiment actually contradicted it, no experiment gave clear support either.

The motivation for this work has been to produce additional low-pressure data in order to obtain an answer to the fundamental question: does the N_2O thermal decomposition reach a low-pressure limit, or does it continue falling off as predicted? The record will show that our data fail to find a low-pressure limit and support the claim of continued falloff at the lowest pressures studied.

TABLE I: Experimental Data on N_2O Decomposition Shown in Figure 1

	author (ref)	diluent, M	concn region, mol/cm^3
△	Johnston (1)	N_2O	low pressure
∔	Kaufman et al. (2)	N_2O	1.6×10^{-7} to 5×10^{-7}
	Lipkea et al. (3a)	Kr	2×10^{-5}
	Zaslonko et al. (3b)	Ar	10^{-5} to 10^{-4}
	Borisov et al. (3c)	Ar	$\sim 10^{-5}$
	Sulzman et al. (3d)	Ar	8×10^{-6} to 3×10^{-5}
	Pamidimukkala et al. (3e)	Ar	6×10^{-6} to 1.5×10^{-5}
	Dean et al. (3f)	Ar	2×10^{-6} to 4×10^{-6}
–	Evaluation of Baulch et al. between 900 and 1500 K (5)	N_2O	1.5×10^{-6} to 8.9×10^{-6}
	Olschewski et al. (13)	Ar	5×10^{-6} to 6×10^{-5}
I	Lindars et al. (5a)	N_2O	2×10^{-7} to 2×10^{-6}
●	Bradley et al. (5b)	Ar	2.2×10^{-6} to 3.8×10^{-6}
	Fishburne et al. (5c)	Ar	1.3×10^{-5}
		O_2	1.1×10^{-5}
	Drummond et al. (5d)	Ar	2.5×10^{-5}
○	Borisov (5e)	Ne	2.1×10^{-6} to 5.7×10^{-6}
	Barton et al. (5f)	Kr	1.4×10^{-6} to 1.8×10^{-6}
	Coleman et al. (5g)	N_2O	4.7×10^{-7} to 3.5×10^{-6}
	Clark et al. (5h)	N_2	2.10×10^{-6}
	Gutman et al. (5i)	Ar	8.10×10^{-7} to 4.5×10^{-6}
×	present work	N_2O	1.5×10^{-6}

2. Experimental Section

The measurements were performed by a static method using conventional gas-handling apparatus.[7] Gas mixtures were introduced through an electromagnetic valve (opening time 30 ms, closing time 20 ms) into a cylindrical quartz vessel (60 mm in diameter and 100 mm long), previously outgassed to 5×10^{-5} torr and kept in a furnace. Temperature was stabilized within ±1 K and was measured with a chromel–alumel thermocouple (0.25 mm diameter) set at the center of the reactor. Pressure change was monitored by a piezoelectric transducer (accuracy 0.04 torr) connected to a strip-chart recorder. When the reaction has proceeded for the desired time, a second electromagnetic valve was opened and the reactants were allowed to expand from the reactor into a bulb at room temperature. Both valves were driven by an electronic timer. The measured gas composition at the longest reaction times corresponded to nearly total conversion.

Sample analyses were carried out by gas chromatography using helium as carrier gas (Porapak Q column at 30 °C). Nitrous

---

(1) H. S. Johnston, *J. Chem. Phys.*, **19**, 663 (1951).

(2) F. Kaufman, J. J. Gerri, and R. E. Bowman, *J. Chem. Phys.*, **25**, 106 (1956).

(3) (a) W. H. Lipkea, D. Milks, and R. A. Matula, *Combust. Sci. Technol.*, **6**, 257 (1973); (b) I. S. Zaslonko, A. S. Losev, and E. V. Mozzhukhin, *Kinet. Katal.*, **21**, 311 (1980); (c) A. A. Borisov and G. I. Skachkov, *Kinet. Katal.*, **13**, 42 (1972); (d) K. G. P. Sulzmann, J. M. Kline, and S. S. Penner, "Proceedings of 12th (International) Symposium on Shock-tubes and Waves", A. Lifshitz and J. Ron, Ed., Magnes, Jerusalem, 1979, p 465; (e) K. M. Pamidimukkala, A. Lifshitz, G. B. Skinner, and D. R. Wood, *J. Chem. Phys.*, **75**, 1116 (1981); (f) A. M. Dean, *Int. J. Chem. Kinet.*, **8**, 459 (1976).

(4) A. J. Lorquet, J. C. Lorquet, and W. Forst, *Chem. Phys.*, **51**, 253, 241 (1980), and references therein.

(5) D. L. Baulch, D. D. Drysdale, and D. G. Horne, "Evaluated Kinetic Data for High Temperature Reactions", Vol. 2 Butterworths, London, 1973, p 69.

(6) W. Forst, *J. Phys. Chem.*, **86**, 1776 (1982).

(7) H. Loirat, D.Sc. Thesis, University of Bordeaux, 1984.

0022-3654/85/2089-4586$01.50/0

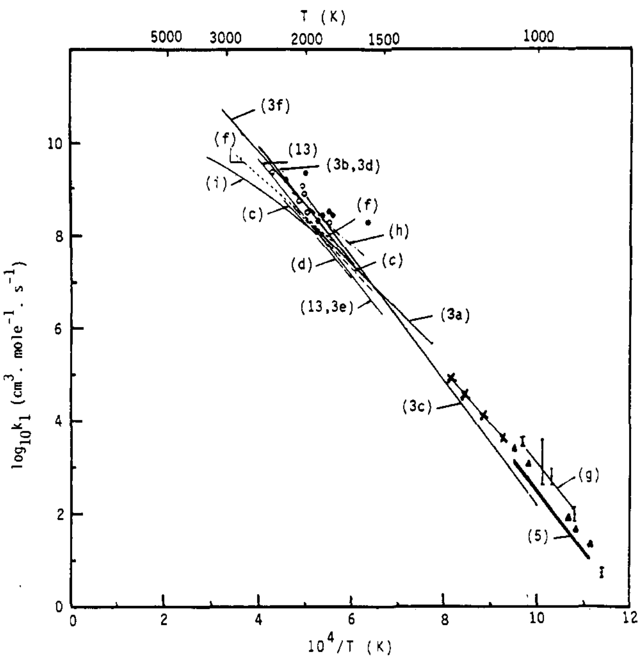

Figure 1. Summary of available experimental data on the decomposition of N_2O. See Table I for identification. Adapted from ref 5.

oxide, carbon dioxide, and nitrogen were obtained from l'Air Liquide (N_2O: purity 99.95%, $H_2O < 20$ ppm, $H_2 < 1$ ppm. CO_2: purity 99.995%, $H_2O < 10$ ppm, $H_2 < 0.1$ ppm. N_2: purity 99.995%, $H_2O < 3$ ppm). N_2O and CO_2 were degassed at 77 K.

The decomposition of nitrous oxide was studied between 1080 and 1020 K by using total gas concentrations in the range 10^{-7} to 1.5×10^{-6} mol/cm^3. Nitrous oxide was used either pure or in two mixtures: mixture 1 consisted of 33% N_2O and 67% CO_2; mixture 2 consisted of 5% N_2O in nitrogen. The time dependence of N_2O, N_2, O_2, and NO concentrations was measured at several temperatures and total gas concentrations. An example of the results of a typical run is shown in Figure 2. It was not possible to work at concentrations much below 10^{-7} mol/cm^3 with the present equipment because of insufficient sample size for chromatographic analysis.

3. Analysis of Experimental Data

The experimental data were analyzed on the basis of the generally accepted mechanism for the decomposition of N_2O, consisting of reactions 1–6. Since experiments were performed

$$N_2O + M \rightarrow N_2 + O + M \qquad (1)$$

$$N_2O + O \rightarrow N_2 + O_2 \qquad (2)$$

$$N_2O + O \rightarrow 2NO \qquad (3)$$

$$O + NO + M \rightarrow NO_2 + M \qquad (4)$$

$$NO_2 + O \rightarrow NO + O_2 \qquad (5)$$

$$NO + N_2O \rightarrow NO_2 + N_2 \qquad (6)$$

$$O + \text{wall} \rightarrow {}^1/_2O_2 + \text{wall} \qquad (7)$$

at low pressures, the heterogeneous wall recombination of oxygen atoms is included (reaction 7). We neglect the reaction $NO_2 + N_2O \rightarrow N_2 + O_2 + NO$ since it is generally believed to be too slow.

The nature of the third body M has to be taken into account even in the decomposition of pure nitrous oxide since M is N_2O at the beginning of the reaction, and mainly $N_2 + O_2$ at the end. Reactions 1a, 1b, and 1c are therefore used in place of reaction

$$N_2O + N_2O \rightarrow N_2 + O + N_2O \qquad (1a)$$

$$N_2O + N_2 \text{ (or } O_2\text{, or NO)} \rightarrow N_2 + O + N_2 \text{ (or } O_2 \text{ or NO)} \qquad (1b)$$

$$N_2O + CO_2 \rightarrow N_2 + O + CO_2 \qquad (1c)$$

1. Thus reaction 1a involves N_2O itself as M, reaction 1b involves diatomic M, and reaction 1c a triatomic M. The analysis of experimental data consisted of fitting computed concentration profiles, obtained from numerical integration of the kinetic rate equations, to experimental concentration profiles by adjusting the values of k_{1a}, k_{1b}, and k_{1c}. Calculations were carried out on a Hewlett-Packard desk-top computer using a Runge–Kutta method.

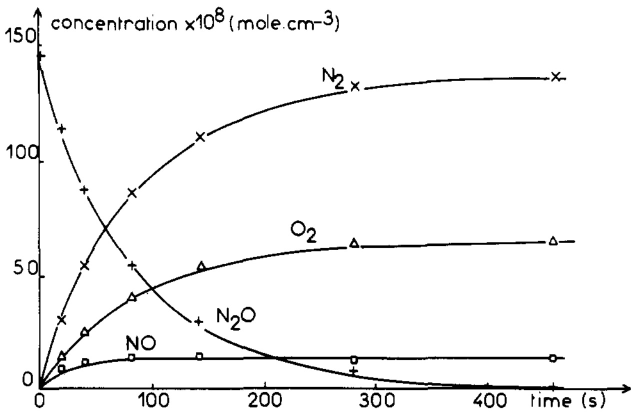

Figure 2. Concentration–time plots for reactant and products in the decomposition of pure N_2O at 10^{-7} mol/cm^3 initial concentration, 1129 K. Points are experimental data; continuous lines are from computer simulation (see text).

The quasistationary state assumption was used for NO_2 and oxygen atoms. Since reaction 1, under our experimental conditions, was always in the pressure-dependent region, the simulation took account of the pressure increase taking place in the course of the decomposition. The following literature values were used for the rate constants of reactions 2–6: $k_2 = 10^{14} \exp(-14100/T)$;[8] $k_3 = k_2/2$;[2,9] $k_5 = 10^{13} \exp(-300/T)$;[5] $k_6 = 2 \times 10^{14} \cdot \exp(-25000/T)$,[10] all in cm^3 mol^{-1} s^{-1}; $k_4 = 1.10 \times 10^{15} \exp(940/T)$ cm^6 mol^{-2} s^{-1}.[5] The evaluation of k_7 for O-atom wall recombination is described below.

Evaluation of O-Atom Wall Recombination. The overall reaction rate of heterogeneous recombination depends on both the molecular diffusion rate (k_{diff}) and the recombination rate on wall surface (k_s). It has been shown[11] that

$$1/k_7 = (1/k_s) + (1/k_{\text{diff}}) \qquad (8)$$

where

$$k_s = \gamma(S/V)(RT/2\pi M)^{1/2} \qquad (9)$$

γ is the recombination coefficient, S/V is the surface:volume ratio of the reactor, M is the molecular mass of reactive species, and

$$k_{\text{diff}} = \left(\frac{\pi^2}{l^2} + \frac{23}{d^2}\right)D \qquad (10)$$

where l and d are the length and diameter of the reactor, respectively; D is the diffusion coefficient which is inversely proportional to the total gas concentration C (given in mol/cm^3 throughout). Under our experimental conditions we have $k_s \simeq 2.5 \times 10^4\gamma$ s^{-1}, $k_{\text{diff}} \simeq 1.3 \times 10^5/C$ s^{-1}.

The value of γ is difficult to estimate. It is generally considered[2,12] to vary between 10^{-2} and 10^{-3}. The values of k_7 calculated for several values of C and γ are given in Table II. (Note that as $\gamma \rightarrow \infty$, $k_7 \rightarrow k_{\text{diff}}$.) For comparison, the rate of the homo-

---

[8] C. P. Fenimore and G. W. Jones, *Symp. (Int.) on Combust.*, [*Proc.*], *8th*, (1962).

[9] W. H. Lipkea, D. Milks, and R. A. Matula, *Combust. Sci. Technol.*, **6**, 257 (1973).

[10] E. S. Fishburne and R. Edse, *J. Chem. Phys.*, **41**, 1297 (1964).

[11] D. A. Frank-Kamenetskii, "Diffusion and Heat Exchange in Chemical Kinetics", Princeton University Press, Princeton, NJ, 1955.

TABLE II

	pure N_2O		mixture 1,
	10^{-7} mol/cm^3	1.5×10^{-6} mol/cm^3	3×10^{7} mol/cm^3
k_7, s^{-1}			
$\gamma \rightarrow \infty$	130	8	40
$\gamma = 10^{-2}$	85	8	35
$\gamma = 10^{-3}$	20	5	15
$\gamma = 10^{-4}$	3		
$(k_2 + k_3)[N_2O]$, s^{-1}			
1070 K	40	600	40
1220 K	150	2250	150

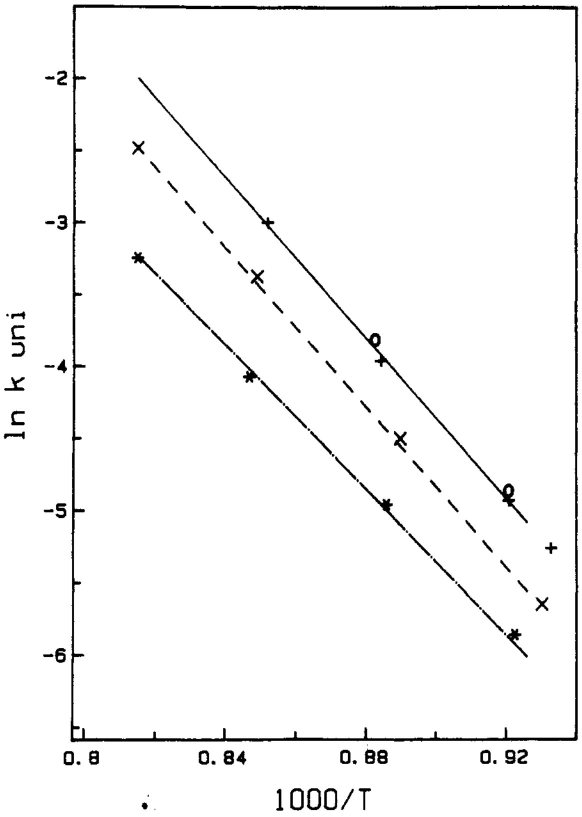

Figure 3. Experimental Arrhenius plots for $\gamma = 10^{-3}$: (* and dot-dashed line) $k_{uni,a}$, 10^{-7} mol/cm^3 (pure N_2O runs); (× and dashed line) $k_{uni,a}$, 3×10^{-7} mol/cm^3 (mixture 1 runs); (+ and continuous line) $k_{uni,b}$, 1.5×10^{-6} mol/cm^3 (pure N_2O runs); (O) $k_{uni,a}$, 1.5×10^{-6} mol/cm^3.

geneous reaction of O atoms is also shown as the bottom entry in Table II. It can be observed that the heterogeneous removal of oxygen atoms is negligible compared to their homogeneous reactions for total gas concentrations above 10^{-6} mol/cm^3, regardless of temperature.

4. Results

The sets of values of k_{1a}, k_{1b}, and k_{1c} were adjusted to obtain the closest fit between experimental and computed concentration–time curves (cf. Figure 2), and k_{uni} was determined as $k_{uni} = k_1C$. In the first case, one obtains values of both $k_{uni,a}$ and $k_{uni,b}$, in the second case values of $k_{uni,a}$, $k_{uni,b}$, and $k_{uni,c}$, and in the third $k_{uni,b}$ only.

Arrhenius plots for experimental results obtained at 1.5×10^{-6}, 3×10^{-7}, and 10^{-7} mol/cm^3 total gas concentration and various temperatures in the range 1072–1227 K are shown in Figure 3 (points); also shown are straight lines from which were obtained activation energies given in Table III (for details see ref 7). Results shown are those for $k_{uni,a}$ using $\gamma = 10^{-3}$ which we believe to be the most reasonable value (also used by Kaufman[2]), except at 1.5×10^{-6} mol/cm^3 where both $k_{uni,a}$ and $k_{uni,b}$ are shown. Since the former was obtained at only two temperatures, we take the activation energy corresponding to $k_{uni,a}$ (O) to be equal to that of $k_{uni,b}$ (+) as represented by the slope of the continuous line in Figure 3.

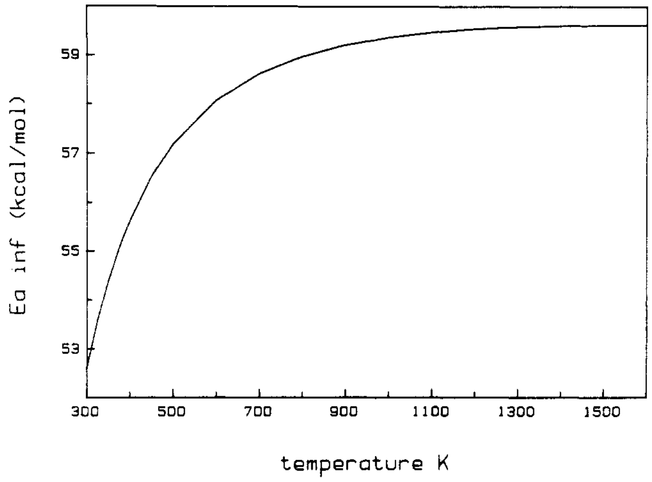

Figure 4. Temperature dependence of limiting high-pressure activation energy $E_{a\infty}$ (eq 13) for N_2O decomposition. Below 600 K $E_{a\infty}$ is calculated from theory, above 1200 K $E_{a\infty}$ is the recommended[5] value (eq 15).

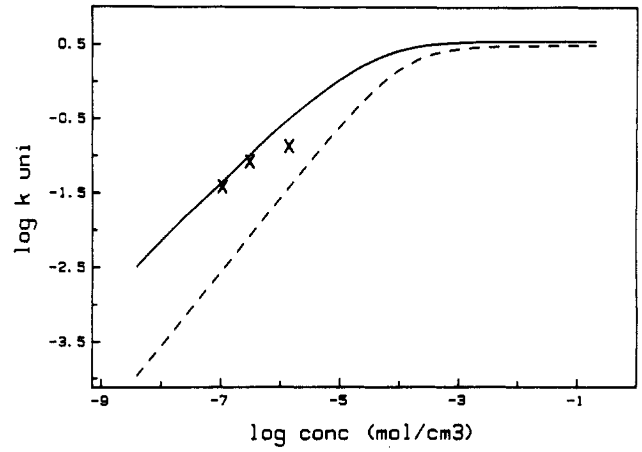

Figure 5. Falloff of general pressure unimolecular rate constant k_{uni} (s^{-1}) for N_2O decomposition at 1227 K. Continuous line: calculated (this work); dashed line: recommended[5] value (eq 20). Points are experimental $k_{uni,a}$ for $\gamma = 10^{-3}$ (uncorrected for heterogeneity).

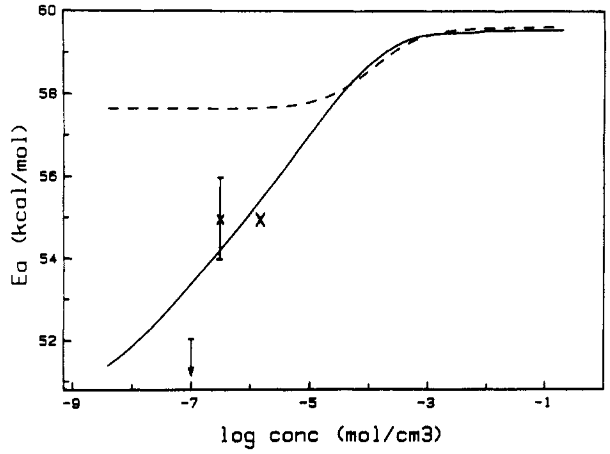

Figure 6. Falloff of general pressure activation energy E_a (eq 19) for N_2O decomposition at 1227 K. Same identification as in Figure 5. Experimental E_a (×) refer to temperature coefficient of $k_{uni,a}$ (uncorrected for heterogeneity). Error bars indicate estimated precision. At the highest concentration, the experimental E_a is only approximate (see text), with a larger probable error than at the other concentrations. At the lowest concentration, the lower limit on the experimental E_a is 48 kcal/mol (Table III) which is outside the graph (arrow). Dashed line is E_a of eq 21.

TABLE III: Results for k_{uni} at Several Temperatures and Concentrations Calculated from Experimental Arrhenius Lines in Figure 3

	temperature, K				
rate constant, s^{-1}	1080	1128	1178	1227	E_a, kcal/mol
Concentration: 1.5×10^{-6} mol/cm^3					
$k_{uni,a}$	6.8×10^{-3}	0.020	0.057	0.145	~55
$k_{uni,b}$	6.1×10^{-3}	0.018	0.051	0.13	55 ± 1
$k_{uni,b}/k_{uni,a}$		~0.9			
Concentration: 3×10^{-7} mol/cm^3					
$k_{uni,a}$ ($k_7 = 35$)	4.35×10^{-3}	0.0125	0.0335	0.0835	53 ± 1
$k_{uni,a}$ ($k_7 = 15$)	3.85×10^{-3}	0.0115	0.0325	0.0835	55 ± 1
$k_{uni,b}/k_{uni,a}$	0.90	0.85	0.80	0.77	-2.9
$k_{uni,c}/k_{uni,a}$	1.0	0.91	0.87	0.87	-2.3
Concentration: 10^{-7} mol/cm^3					
$k_{uni,a}$ ($k_7 = 85$)	3.4×10^{-3}	7.75×10^{-3}	0.0185	0.0405	46 ± 2
$k_{uni,a}$ ($k_7 = 20$)	2.45×10^{-3}	6.6×10^{-3}	0.017	0.0395	50 ± 2
$k_{uni,b}/k_{uni,a}$	0.91	0.83	0.77	0.77	-4.3

TABLE IV: Activation Energies E_a (kcal/mol)

	concentration, mol/cm^3		
	10^{-7}	3×10^{-7}	1.5×10^{-6}
E_a from $k_{uni,a}$ (expt) (Table III)	46 ($\gamma = 10^{-2}$) 50 ($\gamma = 10^{-3}$)	53 ($\gamma = 10^{-2}$) 55 ($\gamma = 10^{-3}$)	55
E_a using Johnston's correction $k_{het} \sim 10^2 \exp(-28000/RT)$	47 ($\gamma = 10^{-2}$) 51.4 ($\gamma = 10^{-3}$)	53.7 ($\gamma = 10^{-2}$) 56.1 ($\gamma = 10^{-3}$)	55.3
E_a calculated (section 6)	53.4	54.2	55.4

Table III summarizes all the data of the present work, recalculated for the same four temperatures at each of the three concentrations by means of the activation energies shown in the rightmost column (error limits are estimated precisions). The data for $\gamma = 10^{-3}$ are plotted in Figures 5 and 6 as a function of concentration.

5. Correction for Heterogeneity

It is well-known that there are surface effects in the thermal decomposition of N_2O, especially at low temperatures and pressures. Johnston,[7] after analyzing two independent sets of data in quartz at 1052 K found that $k_{het} \sim 10^{-4}$ s^{-1}, with an activation energy of $E_{het} = \sim 28$ kcal/mol; thus $k_{het} \sim 10^2 \exp(-28000/RT)$. If the present data are analyzed Johnston's way, it turns out that the plot of k_{uni} vs. concentration extrapolates to $C = 0$ with an obvious nonzero intercept at the lowest temperature (1080 K), which indicates the presence of a heterogeneous contribution, but the intercept decreases appreciably at temperature increases, and is virtually absent at 1227 K, the highest temperature of the present study. Because of insufficient data, this intercept cannot be estimated quantitatively for the purpose of determining the heterogeneous contribution to k_{uni} in this study. However, in order to obtain some estimate of the heterogeneous correction to be applied to the data in Table III, it is possible to proceed in one of several ways.

One is to calculate Johnston's k_{het} at the four temperatures in Table III, and then subtract each k_{het} from the experimental k_{uni}. The difference k_{uni}(expt) − k_{het} then presumably represents the "net" homogeneous k_{uni}. It is then found that the "net" homogenous activation energies at the three concentrations are as shown in Table IV.

Alternatively, we may focus on the lowest concentration of 10^{-7} mol/cm^3 and proceed by assuming that the "net" homogeneous activation energy is 53 kcal/mol, which is the theoretical value calculated for E_a in the next section. It then turns out that this would require that $k_{het} \sim 2.2 \times 10^2 \exp(-28000/RT)$, i.e., a value well within the uncertainty of Johnston's result.

As pointed out in greater detail in the Discussion, our data strongly suggest that the low-pressure limit is not reached even at the lowest concentration studied. If we were to accept the contention of Troe et al.[13] that the N_2O thermal decomposition is already at the low-pressure limit at $\leq 10^{-6}$ mol/cm^3, a reason for our failure to find this limit could be the presence of a heterogeneous component in our measured k_{uni}(expt) at the two lowest concentrations. Assuming, as seems reasonable, that at the highest concentration in this study (1.5×10^{-6} mol/cm^3) the measured k_{uni}(expt) is homogeneous, i.e. substantially free of heterogeneous effects, the (homogeneous) rate constant k_{hom} below this concentration should be a linear function of concentration, if the reaction is indeed at the low-pressure limit, and so k_{hom} can be easily calculated at 3×10^{-7} and 10^{-7} mol/cm^3. The (presumed) heterogeneous component then follows by difference as $k_{het} = k_{uni}(\text{expt}) - k_{hom}$ with the result $k_{het} \sim 2 \times 10^7 \exp(-50000/RT)$. In other words, if it is supposed that we fail to find the low-pressure limit only because of a heterogeneous component in our k_{uni}(expt), it would have to be due to a heterogeneous reaction with the unreasonably high activation energy of ~50 kcal/mol. Moreover, this would lead to the conclusion that at our experimental temperatures the measured rates are almost entirely due to the heterogeneous component. This is contrary to the results near 1000 K of Kaufman[2] et al. who increased the surface area of their quartz vessel by a factor of 40 and found that the rate of the N_2O decomposition increased only slightly.

We conclude therefore that the heterogeneous component in our k_{uni}(expt) does not significantly exceed Johnston's value of k_{het}.

6. Theory

The LLF theory of the nonadiabatic spin-forbidden decomposition of N_2O (eq I) is a nonstatistical theory using a multidimensional model which recognizes explicitly that the N_2O fragmentation proceeds from an initial linear singlet state to a predissociating bent triplet state. From best available potential energy data, the intersection between the linear singlet and bent triplet states is taken to be at 14 135 cm^{-1}, which corresponds to 11 quanta in the N–O stretch; this is the nominal threshold to reaction (E_0) used in all the calculations, including the present one. Franck–Condon factors were computed for the initial–final transition for each oscillator, in the harmonic oscillator approximation, with particular attention to selection rules. The result of the calculations is a set of 126 microcanonical rate constants $k(E)$ for process I at discrete energies E spanning the range from 14 135 to 22 970 cm^{-1}. The driving force for the N_2O dissociation is found to be the flow of energy into the bending vibrations. The calculation of the $k(E)$'s is entirely ab initio with no input from kinetic data except for the spin–orbit coupling constant H^c_{ab}. These microcanonical rate constants $k(E)$ were used in a previous publication dealing with the thermal decomposition[6] of N_2O, with

---

(12) J. C. Greaves and J. W. Linnett, *Trans. Faraday Soc.*, **54**, 1323 (1958); **55**, 1346 (1959); **55**, 1355 (1959); K. Shakhnazaryan, G. A. Sachyan, A. G. Philipossyan, and A. B. Nalbandyan, *Int. J. Chem. Kinet.*, **6**, 693 (1974); D. S. Hacker, S. A. Marshal, and M. Steinberg, *J. Chem. Phys.*, **35**, 1788 (1961); G. Black and T. G. Slanger, *J. Chem. Phys.*, **74**, 6517 (1981).

(13) H. A. Olschewski, J. Troe, and H. Gg. Wagner, *Ber. Bunsenges. Phys. Chem.*, **70**, 450 (1966).

H^c_{ab} adjusted to 10.5 cm^{-1}, which was also used to this study.

In the present instance we propose to use once again the same calculated $k(E)$'s to obtain the thermal rate constant k_{uni} at high temperature, but with an improved calculational technique. The general form of k_{uni} is

$$k_{uni} = \frac{1}{Q}\int \frac{\omega k(E)\, N(E)\, e^{-E/kT}\, dE}{\omega + k(E)} \qquad (11)$$

where ω is the collision frequency, $N(E)$ is the density of states of N_2O at energy E, Q is its partition function at temperature T, and $k(E)$ is the microcanonical rate constant for process I. Unfortunately the calculation of k_{uni} from the theoretical $k(E)$'s is not straightforward because the calculated $k(E)$'s extend only to ~23 000 cm^{-1} which is not high enough to ensure full convergence of the integral in eq 11 at high temperature and arbitrary pressure. "High temperature" here means temperatures in excess of ~700 K, which comprises unfortunately most kinetic studies, the present one included. The reason why no reliable $k(E)$'s can be calculated above 23 000 cm^{-1} has been stated before:[6] cumulative effect of errors in the recursion formula used for calculating Franck–Condon factors, and possible contribution from higher triplet states, which were not considered.

The expedient used to circumvent this problem consists of obtaining the temperature dependence of k_∞, the limiting high-pressure thermal rate constant given by

$$k_\infty = \frac{1}{Q}\int k(E)\, N(E)\, e^{-E/kT}\, dE \qquad (12)$$

from the temperature dependence of the associated activation energy

$$E_{a\infty} = -d \ln k_\infty / d(1/kT) \qquad (13)$$

which can be obtained over a wide temperature range by combining theoretical and experimental data at temperatures where each is most reliable, and then calculating a smooth-function approximation to $k(E)$ from eq 12 by the Laplace transform inversion technique.[14-17] This generates $k(E)$'s at any arbitrarily high energy.

The nonadiabatic spin-forbidden nature of the N_2O decomposition manifests itself in the strong temperature dependence of $E_{a\infty}$ at low temperatures.[15] $E_{a\infty}$ can be obtained reliably below 700 K from the calculated discrete $k(E)$'s by using the discrete summation

$$E_{a\infty} = \frac{\sum_{E_0}^{E=22970} E W'(E)\, k(E)\, e^{-E/kT}}{\sum_{E_0}^{E=22970} W'(E)\, k(E)\, e^{-E/kT}} - \langle E \rangle \qquad (14)$$

where $W'(E)$ is the number of states of N_2O at energy E with at least 11 quanta in the N–O stretch, E_0 is the threshold to reaction (= 14 135 cm^{-1}), and $\langle E \rangle$ is the (thermodynamic) average energy of all the oscillators in N_2O at T. Calculation also shows that $E_{a\infty}$ tends toward a constant limit at high temperature,[6] which, however, cannot be calculated accurately enough. We therefore take for the high temperature limit the "recommended" experimental value[5] for $T \leq 2100$ K

$$k_\infty = 1.3 \times 10^{11} \exp(-20850 \text{ cm}^{-1}/kT) \text{ s}^{-1} \qquad (15)$$

i.e., $E_{a\infty}$ ($T \leq 2100$ K) = 20850 cm^{-1} (= 59.6 kcal/mol), which is then joined smoothly with the low-temperature $E_{a\infty}$ calculated from eq 14, as shown in Figure 4. The curve shown is expressed as least-squares polynomial of eighth order in powers of $1/kT$:

$$E_{a\infty} = \sum_{i=1}^{8} \frac{b_i}{(kT)^{i-1}} \qquad (16)$$

the coefficients [dimension: (cm^{-1})^i] being $b_1 = 20295.1$, $b_2 = 1.445 \times 10^6$, $b_3 = -1.261 \times 10^8$, $b_4 = 4.620 \times 10^{11}$, $b_5 = 1.06 \times 10^{14}$, $b_6 = 1.379 \times 10^{16}$, $b_7 = -9.111 \times 10^{17}$, $b_8 = 2.37 \times 10^{19}$. The expansion in powers of $1/kT$ ensures a better behavior and faster convergence at high temperatures in comparison with the expansion in powers of kT used previously;[15] it also avoids numerical problems in the Laplace inversion.

Integrating (13), making use of the expansion (16), and removing the logarithm yields

$$k_\infty = c \exp\left\{-\sum_{i=1}^{8} \frac{b_i}{i(kT)^i}\right\} \qquad (17)$$

where c is a constant of integration. It is evaluated by comparing, below 600 K, the k_∞ of eq 17 with the "exact" form using the 126 theoretical $k(E)$'s:

$$k_\infty = \frac{\sum k(E)\, W'(E)\, e^{-E/kT}}{\prod_{i=1}^{4} (1 - e^{-h\nu_i/kT})^{-1}} \qquad (18)$$

where the denominator is the quantum mechanical partition function of the four oscillators in N_2O. The result is $c = 1.33 \times 10^{11}$ s^{-1}. With k_∞ of eq 17 now known and used for the left-hand side of eq 12, the Laplace inversion can thus proceed as before, the inverse transform being evaluated by the steepest-descent method.[15,17]

The inversion yields the product function $F(E) = k(E)\, N(E)$ at any number of specified energies E. These were chosen so as to permit direct numerical integration of eq 11 via a 32-point Gauss–Laguerre integration procedure.[18] To obtain $k(E)$ alone (which is required for the denominator of the integrand in eq 11), $F(E)$ must be divided by $N(E)$. In contrast with previous work,[6,15] this density of states was chosen to be that of a N_2O molecule having at least 11 quanta in the N–O stretch, in order to maintain consistency with the basic assumption of the underlying nonstatistical theory. Thus we used throughout $N(E) = G'(E - 14135)/1285$ (cm^{-1})$^{-1}$ (see Appendix), where 1285 cm^{-1} is the frequency of the N–O stretch in N_2O, 14 135 cm^{-1} is the energy of 11 quanta in this oscillator, and $G'(E - 14135)$ is the integrated density of the remaining three oscillators in N_2O at energy $E - 14\,135$ cm^{-1}, evaluated by the method of steepest descents.

While the effect of this substitution for $N(E)$ is negligible at high pressure (cf. eq 12), it yields a better k_{uni} (eq 11) at low pressures. It can be shown[18] that the discrete analogue of eq 11, using the 126 theoretical $k(E)$'s, yields "exact" results (i.e., there is full convergence of the integral) at concentrations below ~10^{-7} mol/cm^3 and at $T \leq 1200$ K, the relevant experimental temperatures in this study. This was used as a benchmark to make sure that k_{uni}, and in particular the associated activation energy

$$E_a = -\frac{d \ln k_{uni}}{d(1/kT)} \qquad (19)$$

obtained by inversion did indeed give back the "exact" result below 10^{-7} mol/cm^3. In fact, concordance of activation energies is a much more sensitive test than concordance of rate constants.

Figures 5 and 6 show the calculated falloff with concentration of k_{uni} and E_a for N_2O decomposition (process I) at 1227 K (continuous lines). The calculation uses for ω the collision frequency based on N_2O–N_2O collisions under Lennard-Jones potential; thus $\omega = CZ_{LJ}$ where $Z_{LJ} = 7.2 \times 10^{13} T^{1/6}$ cm^3/(mol s), and C is concentration in mol/cm^3. Included for comparison is the recommended[5] (ref 5, p 91) falloff curve of k_{uni} for M = Ar, said to be valid between 900 and 2100 K, given by

---

(14) W. Forst, *J. Phys. Chem.*, **76**, 342 (1972); in "Reaction Transition States", J. E. Dubois, Ed., Gordon & Breach, New York, 1972, p 75; *J. Phys. Chem.*, **83**, 100 (1979).

(15) W. Forst, *J. Phys. Chem.*, **86**, 1771 (1982).

(16) W. Forst and S. Turrell, *Int. J. Chem. Kinet.*, **13**, 283 (1981).

(17) C. Schoenenberger and W. Forst, *J. Comput. Chem.*, in press.

(18) C. Schoenenberger, M.Sc. Thesis, Laval University, 1984.

$$k_{\mathrm{uni}} = \frac{1.3 \times 10^{11} e^{-30000/T}}{1 + \dfrac{2.6 \times 10^{4} e^{-1000/T}}{[\mathrm{M}]}} \ \mathrm{s}^{-1} \qquad (20)$$

which is based on experimental data of Olschewski et al.[13] and an interpolation formula of Troe.[18] From eq 20 one can deduce for the activation energy

$$E_{\mathrm{a}} = 59.62 - \frac{5.167 \times 10^{-4} e^{-1000/T}}{[\mathrm{M}] + 2.6 \times 10^{-4} e^{-1000/T}} \ \mathrm{kcal/mol} \qquad (21)$$

Both k_{uni} (eq 20) and E_{a} (eq 21) are shown as dashed lines in Figures 5 and 6, respectively. The figures demonstrate once again[6] that the falloff of activation energy is a much more sensitive indicator of approach to low-pressure limit than rate constant falloff. Since this is an important point in the present context, the following Discussion concentrates exclusively on the concentration dependence of activation energy.

7. Discussion

The dashed (recommended[5]) lines in Figures 5 and 6 are roughly the results one would expect if the only feature of a nonadiabatic spin-forbidden reaction were a smaller than "normal" preexponential factor. Consequently in all other respects the N_2O decomposition is treated as that of a typical "small" molecule, i.e., one that reaches limiting low pressure activation energy at fairly high pressures and shows only a modest falloff of activation energy. While the LLF theory predicts nothing unusual at or near the high-pressure limit (except, possibly, a small preexponential factor), it does predict much different falloff, particularly as regards the activation energy (cf. Figure 6). This has been pointed out before,[6] but the experimental data then available did not offer a clear enough evidence for such a continued falloff.

The present experiments extend the pressure range investigated to pressures almost two orders of magnitude lower than most previous studies. It is noteworthy that the work of Kaufman,[2] although not specifically designed to study the N_2O decomposition rate, also contains information from which can be extracted, albeit somewhat circuitously, low-pressure activation energies 55.7, 55.7, and 51.6 kcal/mol at 1.5×10^{-6}, 3×10^{-7}, and 10^{-7} mol/cm^3, respectively, in reasonably good agreement with our activation energies given in Table III.

It is apparent from the results in Table IV that both the raw experimental data, uncorrected for heterogeneity, and data so corrected show continued falloff of activation energy with concentration. There is no reasonable correction for heterogeneity that would cause the activation energy to even approach a constant limit at low concentrations, much less approach the constant limit of 57.6 kcal/mol, suggested as the recommended[5] limiting low pressure activation energy, supposedly reached below 10^{-6} mol/cm^3. If it is assumed that the reaction is in fact at the low pressure limit below 10^{-6} mol/cm^3, one is then forced to conclude that the measured rate is almost entirely heterogeneous, contrary to experimental evidence. We conclude therefore that the data fail to show any evidence in favor of the thermal decomposition of N_2O reaching a low-pressure limit at pressures as low as 10^{-7} mol/cm^3 and thus give support to the continued falloff of activation energy as predicted by the LLF theory.

When it comes to determining to what extent the calculated falloff curve (continuous line in Figure 6) agrees with experiment, one has to contend with several uncertainties. To begin with, the position of the calculated falloff curve on the concentration axis depends on the assumed collision efficiency, which was taken to be unity, probably a reasonable value for the reactant itself; however, any smaller efficiency would result in a shift of the calculated curve to higher concentrations. In the present case, collision efficiency changes with time as the more efficient N_2O reactant is replaced by less efficient products.

The raw experimental data, uncorrected for heterogeneity, show E_{a} falling off with concentration much more strongly than predicted theoretically, but the exact amount of falloff depends on the assumed value of γ which has a very large effect at the lowest concentration. Since there is an unmistakable heterogeneous component in the reaction, an appropriate correction is in order, which can only be estimated approximately, and thus introduces another uncertainty. On balance, it would appear that theory does in fact underestimate the degree of falloff somewhat.

Finally, the negative activation energies associated with the ratios $k_{\mathrm{uni,b}}/k_{\mathrm{uni,a}}$ and $k_{\mathrm{uni,c}}/k_{\mathrm{uni,a}}$ deserve comment. If we assume that N_2O itself (hence $k_{\mathrm{uni,a}}$) represents a strong collider, these negative activation energies suggest a smaller activation energy for activation with the weaker diatomic ($k_{\mathrm{uni,b}}$) and triatomic ($k_{\mathrm{uni,c}}$) colliders. The difference is about $-RT$ at the two higher concentrations, and about $-1.8RT$ at the lowest, which is in line with calculations[19] which show that the maximum decrease in low-pressure activation energy due to weak collisions is $-2RT$/mol.

Appendix

Density of states for a collection of m harmonic oscillators when one particular oscillator contains at least n quanta.

Let the collection be divided into two groups of oscillators: group 1 that consists of the $m - 1$ oscillators not subject to any restriction as to their content, and group 2 that consists of the one oscillator (frequency $h\nu$) constrained to contain at least n quanta. The total density of states of a system consisting of two parts is quite generally given by the convolution integral[20]

$$N(E) = \int_0^E N_1(E - x)\, N_2(x)\, \mathrm{d}x$$

where $N_1(E - x)$ is the density of states of part 1 at $E - x$ and $N_2(x)$ is the density of states of part 2 at x. In the present case

$$\begin{aligned} N_2(x) &= 0 \qquad \text{if } x < nh\nu \\ &= 1/h\nu \quad \text{if } x > nh\nu \end{aligned}$$

Thus

$$N(E) = (1/h\nu) \int_{nh\nu}^{E} N_1(E - x)\, \mathrm{d}x = (1/h\nu) G'(E - nh\nu)$$

where $G'(E - nh\nu)$ is the total number of states (= integrated density) of the remaining $m - 1$ oscillators at energy $E - nh\nu$, a very good approximation to which is obtainable directly from the steepest-descents formula (6-89) in ref 20 with $k = 1$.

Acknowledgment. W.F. and C.S. are grateful to the National Sciences and Engineering Council of Canada for financial assistance.

Registry No. N_2O, 10024-97-2.

---

(19) J. Troe, *J. Phys. Chem.*, **83**, 114 (1979).

(20) R. C. Battacharjee and W. Forst, *Chem. Phys. Lett.*, **26**, 395 (1974).

(21) W. Forst, "Theory of Unimolecular Reactions", Academic Press, New York, 1973.